MODELING REACTIVE COMPACTION OF HMX

Keith A. Gonthier*
Mechanical Engineering Department
Louisiana State University
Baton Rouge, Louisiana 70803

Mechanically induced heating and ignition of granular HMX due to weak impact is modeled and analyzed. Guided by principles of contact mechanics, bulk dissipated mechanical energy is thermalized at localization sites within the material that are centered at intergranular contact surfaces to estimate compaction induced thermal fluctuations. The evolution of bulk quantities are tracked at the macro-scale, and the evolution of hot-spot temperature and reaction progress are tracked at the grain scale. Model predictions indicate that the onset of sustained combustion occurs for piston speeds that agree well with confined DDT experiments. Results of a parametric study show that the model is reasonably insensitive to variations in key energy localization parameters.

INTRODUCTION

It is well established that thermal energy localization resulting from the rapid deformation of heterogeneous reactive solids, such as propellants, pyrotechnics, and high-explosives, is important for combustion initiation of these materials. Localization occurs at the scale of heterogeneity (i.e., grain scale) due to processes including inelastic grain and binder deformation, intergranular friction, and grain fracture. Importantly, energy localization at the grain scale can have a significant effect on the large scale (bulk scale) material response, possibly triggering detonation [12].

Modeling can be used to characterize the interplay of localized heating and ignition at the grain scale and the system response at the bulk scale. Several bulk models have been developed that describe mechanically induced transition to detonation for both pressed and granular explosives [1, 9, 11]. These models are often only predictive over a narrow range of impact conditions due to inaccurate descriptions of energy localization and ignition. A key goal of this work is the development of a strategy for estimating the magnitude of mechanically induced grain scale thermal fluctuations, important for ignition in heterogeneous solids, within the framework of a continuum-based, bulk model. The strategy requires 1) a model for the bulk material response, 2) a model for the grain scale structure (e.g., grain size, grain packing, etc.), 3) a localization technique for depositing bulk dissipated mechanical energy at the grain scale, and 4) a model for the grain scale response. The grain scale response will allow for the evolution of hot-spot temperature and mass fraction, subject to the localization strategy, rather than imposing their values. Here, it is assumed that the bulk response is experimentally well-characterized and is accurately predicted by the bulk model; as such, we will maintain the integrity of bulk

*Assistant Professor. Email: *gonthier@me.lsu.edu*

model predictions and require that the integrated mass, momentum, and energy of the grain scale model locally equals that given by the bulk model. This constraint is consistent with the common interpretation that the bulk response is an average manifestation of the grain scale response. Models that do not explicitly enforce this constraint may give inconsistent grain scale and bulk predictions. While such a constraint may be restrictive, it does provide a rational framework from which to formulate and explore the implications of various localization strategies.

In this study, some rigor is sacrificed for tractability. Rather than considering PBXs, we focus only on the explosive grains as they are the main compressive load bearing constituent of PBXs. In particular, we model granular HMX because its compaction behavior and DDT have been extensively studied [1, 3, 4, 12, 14]. Experiments indicate that sustained combustion and DDT of confined granular HMX can be triggered by compaction waves resulting from weak mechanical impact (piston speeds $\sim 80 - 90$ m/s) [15]; thus, a fairly well-defined threshold exists for comparing our model predictions against. Other modeling simplifications made in this study are discussed in appropriate sections of this paper.

BULK MODEL

The 1-D bulk compaction model formulated by Gonthier et al [6] is used in this study; the reader is referred there for details. Here, we briefly summarize the bulk model, focusing on issues relevant to compaction induced heating.

The bulk model equations are given by

$$\frac{\partial}{\partial t}\begin{pmatrix}\rho\\ \rho u\\ \rho E\end{pmatrix}+\frac{\partial}{\partial x}\begin{pmatrix}\rho u\\ \rho u^2+P\\ \rho u\left(E+P/\rho\right)\end{pmatrix}=\vec{0}, \quad (1)$$

$$\frac{\partial \phi}{\partial t}+u\frac{\partial \phi}{\partial x}=\frac{\phi\left(1-\phi\right)}{\mu_c}\left(P_s-\beta\right), \quad (2)$$

$$\frac{\partial \tilde{\phi}}{\partial t}+u\frac{\partial \tilde{\phi}}{\partial x}=\begin{cases}\frac{1}{\tilde{\mu}}\left(f-\tilde{\phi}\right) & \text{if } f>\tilde{\phi},\\ 0 & \text{otherwise.}\end{cases} \quad (3)$$

Independent variables in these equations are time t and position x. Dependent variables for the granular solid are density ρ; velocity u; pressure P; total mass specific energy $E = e + u^2/2$, where e is the mass specific internal energy; solid volume fraction ϕ; no-load volume fraction $\tilde{\phi}$; intragranular stress $\beta(\phi, \tilde{\phi})$; and equilibrium no-load volume fraction $f(\phi)$. Quantities associated with the pure phase solid, denoted by subscript "s", are related to the granular solid variables by $\rho_s = \rho/\phi$, $P_s = P/\phi$, and $e_s = e - B$, where $B(\phi - \tilde{\phi}) = \int_0^{\phi'} \frac{\beta}{\rho} d\phi'$ is recoverable compaction energy. The parameters μ_c and $\tilde{\mu}$ appearing in Eqs. (2) and (3) govern the rates of relaxation to the equilibria $P_s = \beta$ and $f = \tilde{\phi}$, respectively. The system of equations is mathematically closed given equations of state $P_s(\rho_s, T)$ and $e_s(\rho_s, T)$, where T is the bulk temperature of the granular solid. In this study, we slightly modify the inert compaction model of Ref. [6] to account for chemical reaction and take $e_s(T, \lambda) = c_v T - \lambda q$, assuming an incompressible solid, where c_v is the specific heat at constant volume, λ is a bulk reaction progress variable that is determined by the grain scale response, and q is the specific heat of reaction. Equation (1) is a system of conservation expressions for the granular solid mass, momentum, and total energy. Equations (2) and (3) are thermodynamically compatible evolution equations for ϕ and $\tilde{\phi}$.

We focus on compaction energetics which is important for the development of the localization model. Because low pressure compaction (< 100 MPa) associated with weak initiation of DDT induces only small density changes, we assume an incompressible solid and ignore compression work. In this case, it can be shown from Eqs. (1-3) that the evolution of internal energy for the granular material is given by

$$\frac{de}{dt} = \frac{de_s}{dt} + \frac{dB}{dt}, \quad (4)$$

where

$$\frac{de_s}{dt} = \frac{\left(P_s - \beta\right)}{\rho}\frac{d\phi}{dt} + \frac{\beta}{\rho}\frac{d\tilde{\phi}}{dt}, \quad (5)$$

$$\frac{dB}{dt} = \frac{\beta}{\rho}\frac{d}{dt}\left(\phi - \tilde{\phi}\right). \tag{6}$$

Here, $d/dt = \partial/\partial t + u\partial/\partial x$ is the convective derivative. Equations (5) and (6) describe the evolution of bulk thermal energy and recoverable compaction energy, respectively. We are particularly interested in Eq. (5) as bulk thermal energy will be deposited at the grain scale based on our localization strategy. Entropy considerations indicate that each term on the right side of Eq. (5) is dissipative.

LOCALIZATION MODEL

We now give 1) a model for the evolution of grain scale material structure, 2) a strategy for localizing bulk dissipated energy at the grain scale, and 3) a model for predicting the grain scale response. The material structure consists of a broad distribution of grain sizes and shapes packed in complex arrangements. Further, experiments indicate that substantial structural changes occur as the material is mechanically loaded [3]. These changes are in large part due to the brittle nature of HMX that readily fractures when compressed. For now, we ignore grain fracture and track the evolution of grain number density $n(x,t)$ by

$$\frac{\partial n}{\partial t} + \frac{\partial}{\partial x}(nu) = 0. \tag{7}$$

We additionally assume that the grains are incompressible and of uniform size and spherical shape; they can be characterized by their constant radii R. Grain number density is related to solid volume fraction and grain size by $n = \phi/(4/3\pi R^3)$. We do not give a detailed description of the grain packing arrangement, but specify the average number of intergranular contact points (surfaces) per grain, γ. For example, a face centered cubic (FCC) arrangement of uniform size spherical grains has $\gamma = 12$, whereas a simple cubic (SC) arrangement has $\gamma = 6$. Though a real granular material will not have such an ordered arrangement, it is reasonable to assume $1 \leq \gamma \leq 16$.

An energy localization strategy should include information based on the dissipative mechanics occurring at the grain scale. Applied bulk loads are transmitted at the grain scale by intergranular contact. Experiments [13] and numerical simulations [2] indicate that the bulk load is not uniformly transmitted through the material, but is preferentially transmitted along certain paths that form stress chains; grains not involved in these chains remain mostly unstressed and inactive. It is reasonable then to expect that grain size, shape, and packing arrangement may have a large effect on the grain scale stress state. The stress state will also depend on the magnitude of the applied load, and possibly the loading rate. For weak loads, the grain scale response will mostly involve localized elastic deformation and friction near active intergranular contact surfaces. In this case, the elastic stress field in the vicinity of a contact can be estimated by Hertz contact theory [10]. The onset of plastic deformation will occur within the grain, near the contact surface, at the location where the principal shear stress, τ, first equals the material yield strength, Y. An expression for τ based on the Hertz solution is given by

$$\tau = \frac{1}{2}P_c\left|(1+\nu)\left[1 - \left(\frac{z}{a}\right)\tan^{-1}\left(\frac{a}{z}\right)\right] - \frac{3}{2}\left[1 + \left(\frac{z}{a}\right)^2\right]^{-1}\right|, \tag{8}$$

where

$$a = \frac{\pi R^* P_c}{2E^*}, \quad R^* = \frac{R}{2}, \quad E^* = \frac{E}{2\left(1-\nu^2\right)}. \tag{9}$$

Here, E is Young's modulus, ν is Poisson's ratio, P_c is the stress at the contact center, and z is distance into the grain normal to the planar, circular contact surface of radius a. We have assumed that contact occurs between spheres of equal size. For axi-symmetric contact, the onset of plastic deformation occurs when $P_c = 1.6Y$, which is based on von Mises' yield criterion. Using the material properties for HMX listed in Table 1, the onset of plastic deformation for a grain size of $R = 25$ μm will occur for $P_c = 0.59$ GPa at a depth $z = 0.45a = 0.93$ μm corresponding to $(\tau)_{\max} = 0.33P_c = 0.2$ GPa. Continued loading will cause the volume of

TABLE 1: HMX MATERIAL PROPERTIES.

Property	*Value*
E, Young's Modulus	24.0 GPa
Y, Yield Strength	0.37 GPa
ν, Poisson's Ratio	0.2
ρ_s, Density	1903.0 kg/m^3
c_v, Specific Heat	1.5 kJ/kg/K
k, Thermal Conductivity	0.502 W/m/K
z, Arrhenius Prefactor	5.0×10^{19} s^{-1}
q, Heat of Reaction	5.95 MJ/kg
T_a, Activation Temperature	2.65×10^4 K

plastically deformed material to increase resulting in plastic flow. Bulk dissipation is the integrated effect of these grain scale dissipative processes.

A phenomenological localization model can be developed based on the foregoing discussion. Because both plastic deformation and friction occur in the neighborhood of intergranular contact surfaces, we track solid regions surrounding these locations within which bulk dissipated mechanical energy will be thermalized; these regions will be referred to as energy localization centers. The number of localization centers per unit volume, $n_c(x,t)$, is related to the number of contact points per grain and grain number density by $n_c = \frac{1}{2}\gamma n$; the prefactor $1/2$ is introduced because each localization center involves contact between two grains. The localization centers are evenly distributed and individually surrounded by solid spheres of radii r_o, where $r_o = R(\frac{1}{2}\gamma)^{\frac{1}{3}}$. The expression for n_c can be combined with the expression for r_o to obtain $n_c = \phi/(\frac{4}{3}\pi r_o^3)$; thus, all solid mass is encompassed by the localization spheres. For an incompressible solid, r_o is constant for a given value of γ. Because grain contact surfaces in real materials would not be evenly distributed, bulk thermal energy would be localized at a fewer number of closely packed localization sites; there may also exist significant thermal interaction between these sites. The present model can indirectly account for increased localization by reducing the value of γ, but does not account for asymmetrical thermal interaction between sites.

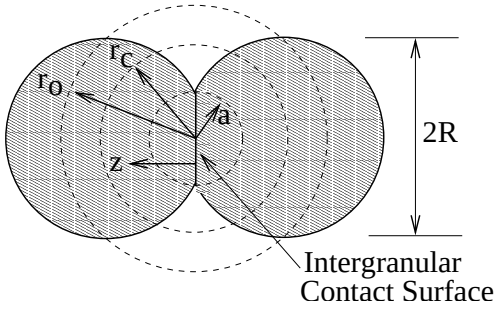

FIGURE 1: LOCALIZATION MODEL GEOMETRY.

Thermal energy will be deposited over a volume of radius $r_c(x,t) \leq r_o$ which defines the localization center, as indicated in Fig. 1. The initial value for r_c is taken as the radius of the intergranular contact surface, a, at the onset of plastic deformation within the grain. This volume is close to the elliptical volume defined by a and the distance from the contact surface at which plastic deformation first occurs, $z = 0.45a$. Thus, we have from the first expression of Eq. (9) that

$$r_c(x,0) = \frac{\pi R^* P_c}{2E^*}, \tag{10}$$

where $P_c = 1.6Y$. This assumption is reasonable in that prior to the onset of plastic deformation most dissipated energy will be due to intergranular friction and will, thus, be localized near the contact surface within the region $r < r_c(x,0)$. To obtain an expression for the evolution of r_c due to material compaction, we assume that the material is perfectly plastic and is in an uncontained mode of plastic deformation. The plastic flow stress is taken to be $P_Y = 3.0Y$ [10]. We equate the volumetric rate of work done by the plastic flow stress to the bulk volumetric dissipated energy given by Eq. (5):

$$n_c P_Y \frac{dV_c}{dt} = \rho_s \phi \frac{de_s}{dt}, \tag{11}$$

where $V_c = \frac{4}{3}\pi r_c^3$ is the localization (plastic) volume for a single sphere. An expression for

the evolution of r_c is thus given by

$$\frac{dr_c}{dt} = \frac{\rho_s \phi}{4\pi r_c^2 n_c P_Y} \frac{de_s}{dt}. \tag{12}$$

Though we have assumed that all bulk dissipated energy is the result of plastic deformation, it can be easily partitioned into both frictional and plastic components; this would involve minimal modification of the model.

The grain scale response tracks the time-dependent, radial evolution of thermal energy and chemical reaction progress of material contained within a single localization sphere subject to thermal energy deposition as discussed above. The approach used here is similar to the modified Frank-Kamenetskii thermal explosion theory of Foster, et al [5]. Evolution equations for thermal energy and reaction progress are given by the following, respectively:

$$\rho_s c_v \frac{d\hat{T}}{dt} = \frac{k}{r^2} \frac{\partial}{\partial r} \left(r^2 \frac{\partial \hat{T}}{\partial r} \right) + q \frac{d\hat{\lambda}}{dt} + \hat{\mathcal{S}}, \tag{13}$$

$$\frac{d\hat{\lambda}}{dt} = z \left(1 - \hat{\lambda}\right) \exp\left(-\frac{T_a}{\hat{T}}\right). \tag{14}$$

Here, r is radial position within the localization sphere. It is necessary to include the convective derivative d/dt because the grains, and thus the localization spheres, locally propagate at the bulk velocity u. Variables labeled with a "hat" ($\hat{\bullet}$) are associated with the localization sphere and vary not only with x and t but also with r; they include solid temperature, $\hat{T}(x,r,t)$, reaction progress, $\hat{\lambda}(x,r,t)$ ($0 \leq \hat{\lambda} \leq 1$, where $\hat{\lambda} = 1$ is complete reaction), and volumetric thermal energy deposition rate $\hat{\mathcal{S}}(x,r,t)$. The grain scale and bulk models will be coupled through the energy source term $\hat{\mathcal{S}}$. Constant parameters contained in Eqs. (13) and (14), and not yet defined, are thermal conductivity, k, Arrhenius prefactor, z, and activation temperature, T_a. Equation (13) is consistent with the caloric equation of state $\hat{e}_s = c_v \hat{T} - \hat{\lambda} q$. Equation (14) models a one-step, irreversible chemical reaction having Arrhenius kinetics. Values for the thermal and chemical parameters for HMX are given in Table 1.

For consistency, we require that the evolution of mass, linear momentum, and thermal energy at the grain scale locally equals that given by the bulk model. It can be easily shown that the mass constraint is identically satisfied. Also, because we are primarily interested in the grain scale thermal energy response, we assume that all grains move at the local bulk velocity; consequently, the linear momentum constraint is trivially satisfied. It remains to satisfy the thermal energy constraint given by

$$\frac{d}{dt}\left(\int_x \rho_s \phi e_s dx\right) = \frac{d}{dt}\left(\int_x \rho_s n_c \, 4\pi \int_0^{r_o} r^2 \hat{e}_s \, dr dx\right). \tag{15}$$

The left hand side of this equation is the evolution of bulk thermal energy for a volume element of arbitrary length in the x-direction. The right hand side of this equation is the evolution of integrated thermal energy at the grain scale. A consequence of this constraint is that the bulk variables T, e_s, and λ are volumetric averages of their corresponding grain scale variables over a localization sphere (e.g., $T = \frac{3}{r_o^3} \int_0^{r_o} r^2 \hat{T} dr$) [8]. Because the localization strategy deposits bulk dissipated energy within localization centers defined by $r \leq r_c$, we take

$$\hat{\mathcal{S}}(x,r,t) = \begin{cases} \left[\dfrac{r_o}{r_c(x,t)}\right]^3 \rho_s \dfrac{de_s}{dt}(x,t) & \text{for } 0 \leq r \leq r_c(x,t) \\ 0 & \text{for } r_c(x,t) < r \leq r_o \end{cases} \tag{16}$$

This expression, while non-unique, with the boundary conditions $\partial \hat{T}/\partial r(x,0,t) = \partial \hat{T}/\partial r(x,r_o,t) = 0$, guarantees that Eq. (15) is identically satisfied.

In summary, the localization model is given by Eqs. (7), (12), (13), and (14), where $\hat{\mathcal{S}}$ is given by Eq. (16), $n_c = \frac{1}{2}\gamma n$, and $r_o = R(\frac{1}{2}\gamma)^{\frac{1}{3}}$. The grain scale model is coupled to the bulk model through the thermal energy equation [Eq. (5)] and the solid volume fraction.

RESULTS

Results are given for localized heating and ignition of granular HMX by steady compaction waves resulting from constant speed piston impact; the analysis is similar to that given by Gonthier and Son [7]. The model equations are solved in a compaction wave-attached frame defined by the transformation $\xi = x - Dt$ and $v = u - D$, where D is the steady speed of a right propagating wave. The analysis is restricted to compaction waves propagating with speeds much less than the ambient solid acoustic speed ($D \ll 3000$ m/s) due to the incompressibility assumption. We also assume that $P_c\tilde{\mu}/\mu_c \ll 1$, where P_c is a characteristic compaction stress; thus, Eq. (3) is replaced by the equilibrium condition $\tilde{\phi} = f(\phi)$. We take $\mu_c = 100$ kg/(s m). For brevity, the constitutive relations for both $f(\phi)$ and $\beta(\phi, \tilde{\phi})$ are not given here, but can be found in Ref. [6]. With these assumptions, the steady problem can be reduced to the following IBVP:

$$\frac{d\phi}{d\xi} = \frac{\phi(1-\phi)}{v\mu_c}\left(P_s - \beta\right), \tag{17}$$

$$\frac{\partial \hat{T}}{\partial \xi} = \frac{\alpha}{vr^2}\frac{\partial}{\partial r}\left(r^2\frac{\partial \hat{T}}{\partial r}\right) + \frac{q}{\rho_s c_v}\frac{\partial \hat{\lambda}}{\partial \xi} + \frac{\hat{\mathcal{S}}}{\rho_s c_v v}, \tag{18}$$

$$\frac{\partial \hat{\lambda}}{\partial \xi} = \frac{z}{v}\left(1-\hat{\lambda}\right)\exp\left(-\frac{T_a}{\hat{T}}\right), \tag{19}$$

$$\frac{dr_c}{d\xi} = \frac{(P_s - \beta) + f'\beta}{4\pi r_c^2 n_c P_Y}\frac{d\phi}{d\xi}, \tag{20}$$

where $\alpha = k/(\rho_s c_v)$ and $f' = df/d\phi$. We have substituted Eq. (5) into Eq. (12), with $\tilde{\phi} = f$, to obtain Eq. (20). Initial conditions for the unstressed granular solid are $\phi(0) = 0.655$, $\hat{T}(0,r) = 300$ K, $\hat{\lambda}(0,r) = 0$, and $r_c(0) = 1.6\pi R^* Y/(2E^*)$. Boundary conditions for the grain scale model are $\partial\hat{T}/\partial r(\xi, 0) = \partial\hat{T}/\partial r(\xi, r_o) = 0$. The system of PDEs is numerically solved by a MOL technique using an implicit, stiff ODE solver. To this end, the radial coordinate of the localization sphere is discretized into 100 evenly spaced nodes and the radial derivative in Eq. (18) is approximated by a second-order accurate centered finite-difference relation.

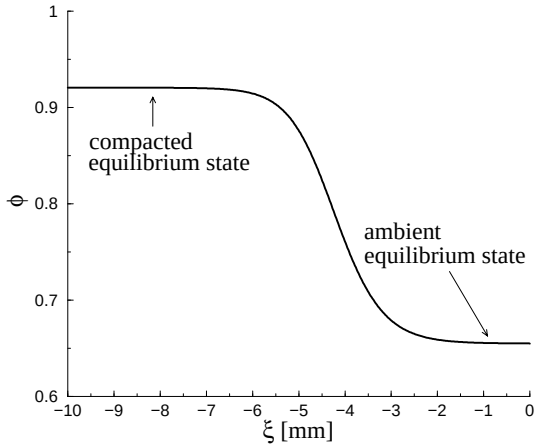

FIGURE 2: COMPACTION ZONE PREDICTION FOR SOLID VOLUME FRACTION ($u_p = 85.6$ m/s).

We first give predictions for the localized heating of inert HMX (i.e., for $\hat{\lambda} \equiv 0$) for $u_p = 85.6$ m/s, and then consider reactive HMX for this same value of u_p. This piston speed is chosen because it is close to that needed for the predicted onset of sustained combustion. The corresponding compaction wave speed is $D = 297.5$ m/s. The values $R = 25$ μm and $\gamma = 12$ are used as representative of lightly compacted granular HMX. The variation of ϕ within the compaction zone for both of these simulations is given in Fig. 2.

Inert Compaction

Figure 3 gives predictions of the energy localization model for heating within the compaction zone of inert HMX. Though not shown here, grain number density smoothly increases from its initial value of $n = 1.11 \times 10^7$ grains/cm^3 to an equilibrium value of 1.41×10^7 grains/cm^3 through the wave as the material is compacted. The equilibrium value for the number of energy localization sites is $n_c = \frac{1}{2}\gamma n = 8.46 \times 10^7$ sites/cm^3. Compaction induces mechanical energy dissipation within material contained by localization cen-

ters that individually surround grain contact points. The spherical volume of material contained within a localization center, characterized by its radius r_c, increases from its initial value of $r_c = 0.93$ μm to a final value of 2.55 μm due to plastic flow. The outer radius of the localization sphere remains constant at $r_o = 13.76$ μm because the solid grains are incompressible. A pulse-like volumetric heat deposition rate is predicted for the localization center, reaching the maximum value $\hat{\mathcal{S}} = 0.52$ GW/cm^3 within the compaction zone where $\phi = 0.73$ at $\xi = -3.71$ mm. Though this rate is high, it is well below the characteristic heat generation rate of approximately $\hat{\mathcal{S}}_d = \rho_s q D_d / L_d = 3.1 \times 10^4$ GW/cm^3 (for $D_d =$ 7000 m/s and $L_d = 2.55$ μm) that would be associated with detonation of the solid HMX contained within the localization center. This heating gives rise to the temperature field of Fig. 3(b). The plot shows radial temperature profiles within a localization sphere though the compaction zone. A maximum temperature of 735.5 K is predicted at the center of the localization sphere at $\xi = -4.69$ mm; thus, the peak temperature within the compaction zone trails the peak energy deposition rate. The temperature rapidly decreases as the applied energy deposition rate vanishes. Though not shown here, the temperature field within the localization sphere approaches the uniform bulk value of $T = 302.4$ K as $\xi \to -\infty$. This feature is a consequence of having energetically consistent localization and bulk models.

Figure 3 indicates that much of the applied thermal energy remains in the vicinity of the localization center through the compaction wave as there is little time for conduction into the cooler grain interior. This observation does not imply that thermal conduction is unimportant in the heating process. An estimate for the change in temperature of material contained in the localization center in the absence of thermal conduction is given by $\Delta T = \hat{\mathcal{S}}_{avg} \mathcal{T} / (\rho_s c_v)$, where $\hat{\mathcal{S}}_{avg}$ and $\mathcal{T}$ are the average applied energy deposition rate and grain residence time within the compaction zone, respectively. Taking $\hat{\mathcal{S}}_{avg} = 0.2$ GW/cm^3 and $\mathcal{T} = 19$ μs, which are characteristic of the predictions shown here, then $\Delta T = 1331$ K. Indeed, the same simulation performed with $\alpha = 0$ m^2/s predicts a temperature within the localization center that is in excess of 1400 K.

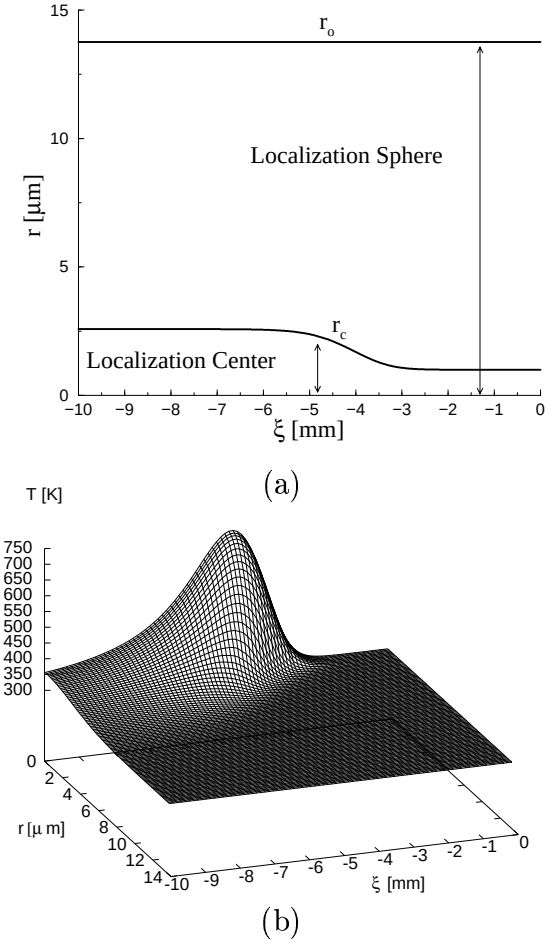

FIGURE 3: LOCALIZED HEATING PREDICTIONS FOR INERT HMX ($u_p = 85.6$ m/s): (a) LOCALIZATION CENTER, (b) HOT-SPOT TEMPERATURE.

Reactive Compaction

Figure 4 gives predictions of the energy localization model for heating and chemical reaction within the compaction zone of HMX. Profiles for n, n_c, r_c, r_o, and $\hat{\mathcal{S}}$ are the same as those for the inert case. The predicted variation through the compaction zone of the radial temperature profile within a localization

sphere is shown in figure (a); the corresponding variation in local reaction progress is shown in (b). The temperature near the center of the sphere is sufficient to induce chemical reaction that locally goes to completion ($\hat{\lambda} = 1$). The reaction accelerates almost to the point of thermal explosion as indicated by the presence of a sharp temperature spike. However, thermal energy conduction from the reaction site into the grain interior freezes the reaction causing a rapid decrease in temperature. A peak temperature in excess of 1200 K is predicted prior to extinction of chemical reaction. Only a small fraction of the total mass is heated to elevated temperatures, and its thermal inertia is insufficient to overcome thermal conduction losses and achieve sustained combustion.

For this simulation, $u_p = 85.6$ m/s. Numerical experiments indicate that this piston speed is close to the thermal explosion threshold; the value $u_p = 85.7$ m/s results in a thermal explosion marking the onset of sustained combustion of the material. This prediction agrees well with the results of confined DDT tube tests involving piston impact of granular HMX [12, 15]. These tests indicate that the explosion is first triggered for piston speeds approximately in the range $80 \leq u_p \leq 90$ m/s. Combustion is often observed for piston speeds slightly below this threshold, but transition to detonation does not occur.

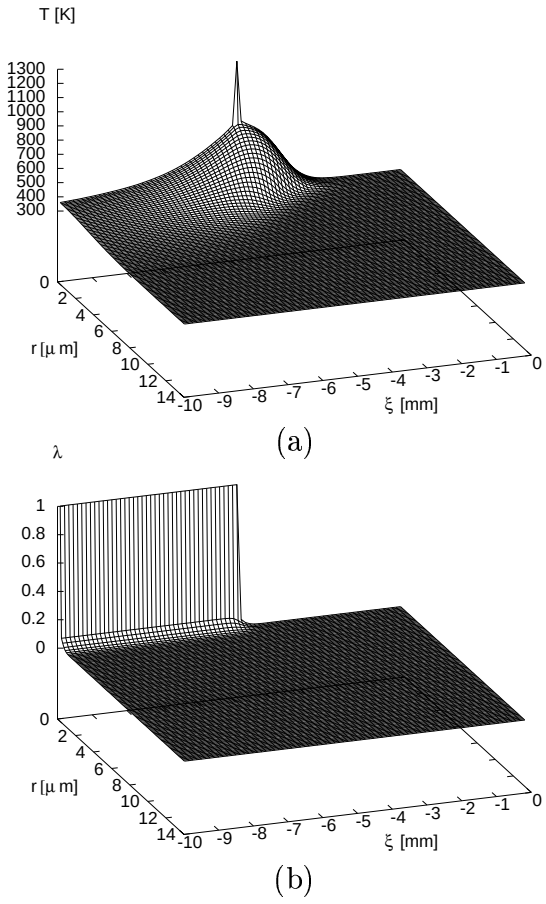

FIGURE 4: PREDICTED HOT-SPOT (a) TEMPERATURE AND (b) REACTION PROGRESS ($u_p = 85.6$ m/s).

Parametric Sensitivity

Numerical experiments were performed to determine the model sensitivity to variations in key energy localization parameters. To this end, parameter values used for the reactive compaction simulation were chosen as a baseline, and the values of γ and P_Y/Y were independently varied over physically significant ranges. The piston speed needed for sustained combustion (thermal explosion) was determined for each case. Here, the value of γ determines the hot-spot density of the mesostructure and the ratio P_Y/Y determines the growth rate of r_c, given by Eq. (12). Both of these parameters control the volume over which bulk dissipated energy is localized. Because grain size is an important, easily adjustable system parameter, its influence on the predicted onset of sustained combustion was also determined.

Results of the sensitivity analysis are summarized in Fig. 5. The value of γ was varied over the range $1 \leq \gamma \leq 14$; it is reasonable to expect that, on average, the number of contact points per grain lies within this range. The predicted threshold for sustained combustion increases with γ as bulk dissipated energy is distributed over a larger material volume. The value of P_Y/Y was varied over the range $1.6 \leq P_Y/Y \leq 6.0$ which is typical of contact problems [10]. The sustained combustion threshold is predicted to decrease with increasing P_Y/Y as bulk dissipated energy is localized over smaller material volumes. Impor-

tantly, these predictions do not deviate significantly from the experimentally observed explosion threshold for granular HMX. This result suggests that the localization strategy used in this study may be a viable approach to develop improved mechanical ignition models based on grain scale thermal fluctuations.

Lastly, the influence of grain size on the predicted combustion threshold is shown in Fig. 5(d). Here, it is seen that the piston speed for sustained combustion rapidly increases as grain size decreases. A value of $u_p = 384.2$ m/s is needed to trigger sustained combustion for a material composed of $R = 2.5$ μm size grains. This result agrees with experimental observations which show the same trend. Further, the necessary piston speed decreases only slightly for grains having approximately $R > 30$ μm.

CONCLUSIONS

Predictions for mechanically induced hot-spot formation and ignition of granular HMX that is associated with the weak initiation of DDT were described in this paper. To this end, a bulk compaction model was coupled with a grain scale model that tracked the evolution of hot-spots within the material meso-structure. Importantly, the interplay between localized energy deposition, thermal conduction, and chemical reaction at the grain scale was resolved. The deposition of bulk dissipated energy in the vicinity of intergranular contact surfaces was guided by contact mechanics. The bulk and grain scale models were coupled in an energetically consistent manner that preserved the integrity of the experimentally correlated bulk predictions.

Localized heating predictions indicate that temperatures sufficient to induce chemical reaction can result from weak piston impact. Temperatures near 700 K were predicted for piston speeds near 86 m/s, the value needed for the onset of sustained combustion. This result agrees well with experimentally determined explosion thresholds for granular HMX. Also, thermal conduction was shown to have a significant influence on the ignition process; in the absence of thermal conduction, excessively high temperatures were predicted near intergranular contact points. Predictions showing the model response to variations in key energy localization parameters indicate that it is reasonably insensitive to the localization strategy. This study suggests that mechanically induced ignition can be accurately predicted if important meso-scale features responsible for thermal fluctuations are resolved.

ACKNOWLEDGMENTS

This work was supported by a 2001 NRC/AFOSR Summer Faculty Fellowship. Both Capt. Keith M. Roessig, Ph. D., and Dr. Joseph C. Foster, Jr., AFRL/MNMW, are gratefully acknowledged for their assistance in this work.

REFERENCES

[1] Baer, M. R., and Nunziato, J. W., "A Two-Phase Mixture Theory for the Deflagration-to-Detonation Transition in Reactive Granular Materials," *Int. J. Multiphase Flow*, Vol. 12, 1986, pp. 861-889.

[2] Bardenhagen, S. G., and Brackbill, J. U., "Dynamic Stress Bridging in Granular Material," *J. Appl. Phys.*, Vol. 83, No. 11, 1998, pp. 5732-5739.

[3] Burnside, N. J., Son, S. F., and Asay, B. W, "Thick Walled DDT Tube Experiments," JANAF PSHS Meeting, Naval Postgraduate School, Nov. 4-8, 1996.

[4] Coyne, P. J., Elban, W. L., and Chiarito, M. A., "The Strain Rate Behavior of Coarse HMX Porous Bed Compaction," Proc. 8th Detonation Symp., 1989, pp. 645-657.

[5] Foster, J. C., Jr., Christopher, F. R., Wilson, L. L., and Osborn, J., "Mechanical Ignition of Combustion in Condensed Phase High Explosives," *Shock Compression of Condensed Matter*, 1997, pp. 389-392.

[6] Gonthier, K. A., Menikoff, R., Son, S. F., and Asay, B. W., "Modeling Compaction Induced Energy Dissipation of Granular HMX," Proc. 11th Detonation Symp., 1998, pp. 153-161.

[7] Gonthier, K. A., and Son, S. F., "Modeling Compaction Induced Energy Localization in Granular HMX," *Shock Compression of Condensed Matter*, 1999, pp. 393-396.

[8] Gonthier, K. A., "Modeling and Analysis of Reactive Compaction for Granular Energetic Solids," AFRL-MN-EG-TR-2001-7091, Air Force Research Laboratory, 2001.

[9] Johnson, J. N., Tang, P. K., and Forest, C. A., "Shock-Wave Initiation of Heterogeneous Reactive Solids," *J. Appl. Phys.*, Vol. 57, No. 9, 1985, pp. 4323-4334.

[10] Johnson, K. L., *Contact Mechanics*, Cambridge University Press, New York, 1985.

[11] Massoni, J., Saurel, R., Baudin, G., and Demol, G., "A Mechanistic Model for Shock Initiation of Solid Explosives," *Phys. Fluids*, Vol. 11, No. 3, 1999, pp. 710-736.

[12] McAfee, J. M., Asay, B. W., Campbell, W., and Ramsay, J. B., "Deflagration to Detonation Transition in Granular HMX," Proc. 9th Detonation Symp., 1989, pp. 265-278.

[13] Roessig, K. M., and Foster, J. C., Jr., "Experimental Simulations of Dynamic Stress Bridging in Plastic Bonded Explosives," *Shock Compression of Condensed Matter*, 2001.

[14] Sandusky, H. W., and Liddiard, T. P., "Dynamic Compaction of Porous Beds," NSWC Report, No. 83-246, 1985.

[15] Son, S. F., and Burnside, N. J., private communication, 1998.

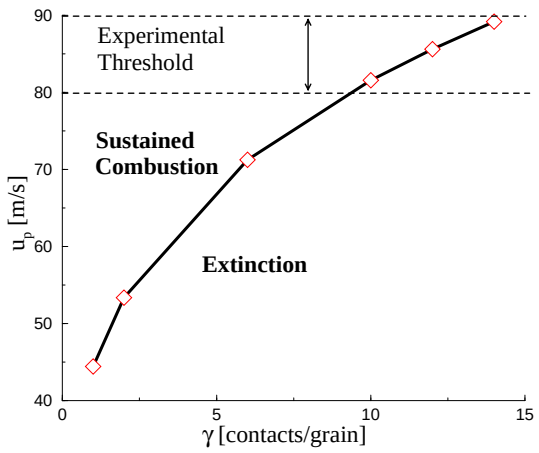

(a)

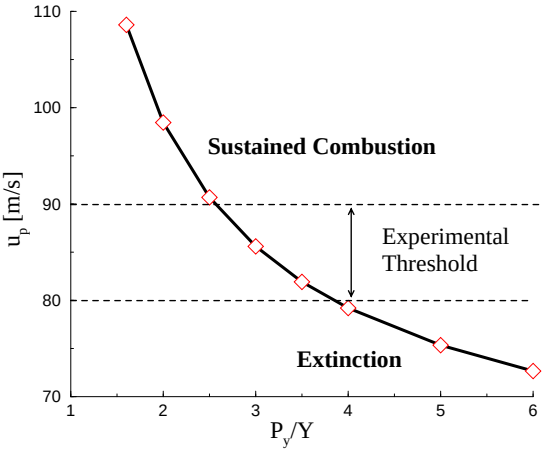

(b)

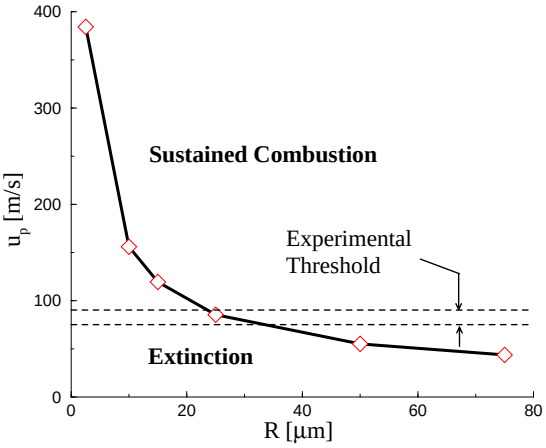

(c)

FIGURE 5: SENSITIVITY RESULTS: (a) CONTACTS/GRAIN, γ; (b) LOCALIZATION CENTER GROWTH RATE, CHARACTERIZED BY P_Y/Y; (c) GRAIN SIZE, R.